FDTD ANALYSIS OF A SIZED-REDUCED, DUAL-FREQUENCY PATCH ANTENNA

S. Gao

Department of Communications Engineering
Shanghai University
Jiading, Shanghai, 201800, P.R. China

J. Li

Department of Computer Science
Nanjing University
Nanjing, 200000, P.R. China

1. INTRODUCTION

Many applications in communications and radar systems often require the antennas with dual-frequency capabilities. The dual-frequency operations include two different cases, which are antennas working in dual bands but with orthogonal polarizations and that with same polarizations. Both cases are very useful for different applications.

The dual-frequency operation with same polarizations can be obtained by using stacked geometry or coplanar parasitic structures [1–4]. It can also be obtained by loading the antenna with reactive lumped or distributed elements [5–9]. Another kind of reactive loading can be introduced by etching slots on a patch [10, 11]. The antenna proposed in [10] is a rectangular patch with two very narrow slots etched close and parallel to the radiating edges. A combination of slots loading and short circuits is presented in [12].

Designs of the dual-frequency antennas with orthogonal polarizations are reported recently [13–15]. In these designs, the two operating frequencies are the resonant frequencies of the TM_{01} and TM_{10}, modes of the rectangular microstrip patch, which are of orthogonal polarization planes, and can be excited using a single probe feed or an inclined-slot-coupling feed. An experimental study is presented in [15], where a square slot is proposed to be cut in the center of the rectangular patch to realize dual- frequency antenna with an antenna-size reduction of $\sim 17\%$. However, with this antenna, no further size reductions are possible due to the poor impedance matching characteristics at both bands, as stated in [15]. To realize greater antenna-size reduction, a 45°-rotated square slot is also proposed in [15]. However, no significant improvement is observed.

In this paper, the rectangular slot is proposed to be cut in the center of the rectangular patch instead of the square slot. To get full-wave results, the FDTD method is developed to analyze the characteristics of the rectangular patch antenna with a rectangular slot cut in the center. A simple and accurate model is proposed for the probe feed. A simple method of calculating the radiation patterns is also presented. The electric current distributions on the rectangular patch for both the rectangular slot loaded case and the case without slot are presented, together with the radiation patterns. It is shown that by cutting a rectangular slot in the center and proper location of the feed point, large reduction of the patch size with good impedance matching characteristics at both bands could be realized easily by tuning the length and width of the slot and patch. The example presented in this paper achieves an antenna-size reduction of $\sim 33\%$.

In section 2, the FDTD method used in present analysis is described, with emphasis on the feed model and the method of calculating the radiation patterns. The numerical results of the dual-frequency antennas are presented in section 3, together with discussions. The comparisons
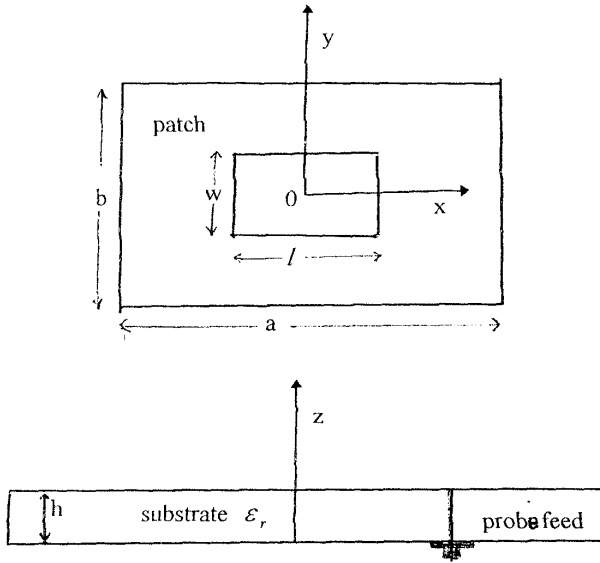
Figure 1. Geometry of rectangular microstrip antenna with a rectangular slot.

with experimental results are also presented. Conclusions are drawn in section 4.

2. FDTD METHOD

2.1 Outline of FDTD Method

Figure 1 shows the rectangular patch antenna loaded with a rectangular slot in the center. For the rectangular patch, the length and width are denoted by a and b respectively. The length and width of the rectangular slot are denoted by l and w respectively. (X_s, Y_s) is the coordinate of the probe feed.

The FDTD (finite difference time domain) method has been widely applied to analyze the electromagnetic performance of antennas and microwave devices. With transient excitation, it provides impedance and scattering parameters over a wide frequency band with one calculation and application of the fast Fourier transformation (FFT). The basic principles of the FDTD method have been well documented in [16–20]. Here, only the main procedures used in this paper are

presented. The emphasis here is on the feed model and the calculation of radiation patterns.

A Gaussian pulse with unit amplitude, given by

$$V(t) = e^{-\frac{(t-t_0)^2}{T^2}} \tag{1}$$

is excited in the probe feed. The dimensions of the FDTD unit cell, Δx, Δy, Δz, are chosen such that integral number of nodes can fit exactly all the dimensions of the patch antenna. To accurately model the spatial variation of field in the slot, the unit cell dimensions are also constrained to a fraction of the slot length and width under consideration. We find it necessary to maintain at least 20 spatial steps per wavelength for accurate results. The maximum time step is chosen according to Courant stability criterion. The metal conductors are assumed to be perfect conductors with zero thickness, modeled by setting the tangential electric field components on this plane to be zero. At the air-dielectric interface, the average of the two dielectric constants $\frac{\varepsilon_r+1}{2}$ is used. After the excitation is launched, the fields are computed at successive time steps until all of the field intensities in the domain decay to a negligible steady-state value. To truncate the infinite space, the absorbing boundary conditions used are the combination of the third order Liao's ABC's and the super absorbing techniques [21, 22].

2.2 Probe Feed Model

The accurate modeling of the source feed excitation is very important for the FDTD analysis of microstrip antennas. It is more difficult to model the probe feed than the microstrip line-fed case. A number of papers have been reported on the probe-feed model. The model in [18, 23] is an ideal voltage generator connected to the source resistor and the input impedance of the antenna. In [24], a portion of the coaxial probe terminated in an absorbing boundary is included in the FDTD calculation. The absorbing boundary helps dissipate energy reflected back to the source. A more complicated model is proposed in [25], where the curved boundary of the inner and outer conductors of a coaxial line is approximated by staircasing, and the tangential electric field components are forced to be zero at the conductor surface. This model takes into account of the contributions from the higher order modes at the junction between the probe and the antenna. However, it is more cumbersome than the simple gap-feed model.

In this paper, a simple extension to the gap-feed model proposed in [18, 23, 30] is presented. The feed model is shown in Figure 2. Note in this case the substrate height is equal to $3\Delta z$ and the series resistor R_s is assumed to be $50Q$. By applying Ampere's circuital law, the current on the feed probe is obtained by taking the line integral of magnetic field around the electric field source location, which is given as

$$
\begin{aligned}
I^{n-\frac{1}{2}} =& \left[H_x^{n-\frac{1}{2}}(i_s, j_s - 1, k_s + 1) - H_x^{n-\frac{1}{2}}(i_s, j_s, k_s + 1) \right] \Delta x \\
&+ \left[H_y^{n-\frac{1}{2}}(i_s, j_s, k_s + 1) - H_y^{n-\frac{1}{2}}(i_s - 1, j_s, k_s + 1) \right] \Delta y \quad (2)
\end{aligned}
$$

By applying Ohm's law to the circuit of Figure 2(a), the electric source field is obtained as

$$
E^n(i_s, j_s, k_z) = \frac{V(n\Delta t) + I^{n-\frac{1}{2}} R_s}{3\Delta z} \quad (3)
$$

where $k_z = k_s$, $k_s + 1$, $k_s + 2$. Finally, the current and voltage are transformed to the Fourier domain. The input impedance of the antenna is obtained from

$$
Z_{in} = \frac{V(f)}{I(f)} - R_s \quad (4)
$$

2.3 Calculation of Electric Current Distributions on the Patch

To get the electric current distributions on the patch, a sinusoidal excitation at probe feed is used, which is given by

$$
V(t) = \sin 2\pi f_0 t \quad (5)
$$

where f_0 is the resonant frequency of interest. The feed model is same as before. The field distributions on the patch are recorded at one instant of time after steady state has been reached. In our analysis, the total time for stability is more than 8 cycles. The electric current distributions on the patch are given by

$$
\begin{aligned}
J_x(i, j, k_s + 2) &= - \left[H_y(i, j, k_s + 3) - H_y(i, j, k_s + 2) \right] \\
J_y(i, j, k_s + 2) &= H_x(i, j, k_s + 3) - H_x(i, j, k_s + 2)
\end{aligned} \quad (6)
$$
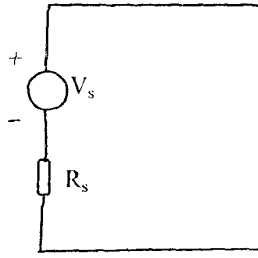
(a)
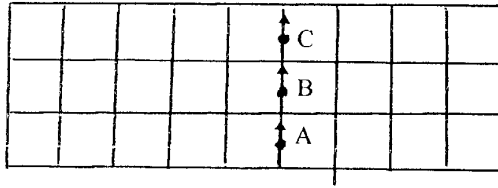
$A(i_s, j_s, k_s)$, $B(i_s, j_s, k_s+1)$, $C(i_s, j_s, k_s+2)$

(b)

Figure 2. The probe feed model.

2.4 Calculation of the Radiation Patterns

In [18, 23, 26], methods have been proposed to obtain the far-field radiation patterns from the FDTD simulation. According to these methods, firstly, a surface has to be defined which surrounds the antenna in three dimensions. A sinusoidal excitation near the resonant frequency is used, and the electric and magnetic fields on the enclosing surface are recorded at one instant of time after the fields reach steady state. A set of equivalent electric and magnetic currents can be deduced from the magnetic fields and electric fields respectively. The Hertz potentials are derived from the equivalent currents and the radiation patterns are obtained by using the radiation equation [27].

A simpler method is proposed here, which combines the time domain computations and the methods in the frequency domain [28]. Only the electric current distributions on the patch are needed, which are easily obtained from (6). The expressions for far fields are

$$E_\theta(\theta,\phi) = \widetilde{E}_x(k_x, k_y, k_s + 2)\cos\phi + \widetilde{E}_y(k_x, k_y, k_s + 2)\sin\phi$$

$$E_\phi(\theta,\phi) = \widetilde{E}_x(k_x, k_y, k_s + 2)\sin\phi - \widetilde{E}_y(k_x, k_y, k_s + 2)\cos\phi$$

$$\begin{bmatrix} \widetilde{E}_x \\ \widetilde{E}_y \end{bmatrix} = \begin{bmatrix} \widetilde{G}_{xx}^{EJ} & \widetilde{G}_{xy}^{EJ} \\ \widetilde{G}_{yx}^{EJ} & \widetilde{G}_{yy}^{EJ} \end{bmatrix} \begin{bmatrix} \widetilde{J}_x \\ \widetilde{J}_y \end{bmatrix} \tag{7}$$

$$\begin{bmatrix} \widetilde{J}_x \\ \widetilde{J}_y \end{bmatrix} = \iint_{S\rho} \begin{bmatrix} J_x \\ J_y \end{bmatrix} \cdot e^{j(k_x x + k_y y)} dxdy$$

where $k_x = k_0 \sin\theta \cos\phi$ and $k_y = k_0 \sin\theta \sin\phi$. $\widetilde{G}_{xx}^{EJ}, \widetilde{G}_{xy}^{EJ}, \widetilde{G}_{yx}^{EJ}, \widetilde{G}_{yy}^{EJ}$ are dyadic Green's functions in spectral domain, which are available in [28].

3. NUMERICAL RESULTS

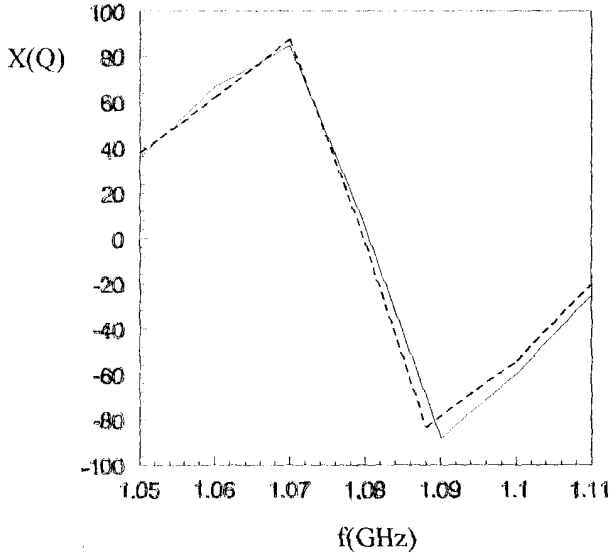### 3.1 Comparisons with Experimental Results

To verify the FDTD programs developed here, a lot of comparisons are made between available experimental results of slot-loaded antennas and FDTD simulation. Good agreement is observed in all cases and only two examples are presented here. Figure 3 shows the comparisons between experimental results of the rectangular ring antenna in [29] and our results. The comparisons between experimental results in [15] nd FDTD results are shown in Figure 4. The theoretical and experimental results are very close. These comparisons give us confidence in our FDTD programs.

3.2 Numerical Results and Discussions

Figure 5 shows the input return loss of the rectangular patch antenna loaded with a rectangular slot in the center. The feed point is at (1.05 cm, 1.25 cm). The two resonant frequencies of the antenna are 1.54 GHz and 2.50 GHz respectively. The two resonant frequencies of the simple antenna without slot are 2.115 GHz and 2.698 GHz. It is seen that the two frequencies are lowered by $\sim 27\%$ and $\sim 9\%$ respectively. This corresponds to an antenna-size reduction of $\sim 33\%$ for a fixed dual-frequency operation using the present proposed design instead of using the simple-patch design in [13]. The square-slot
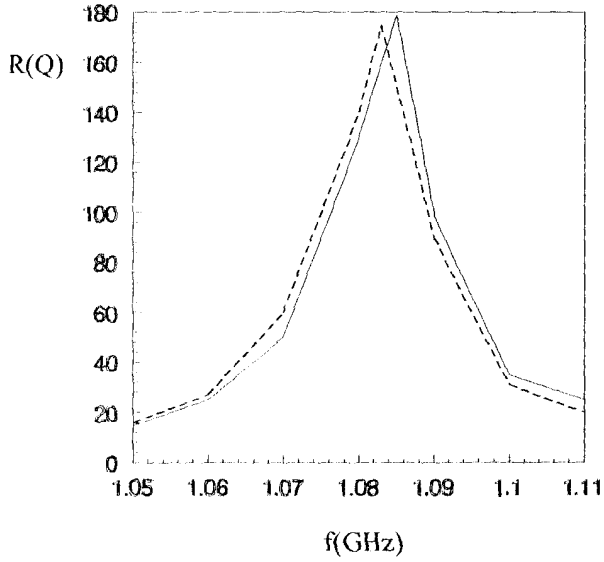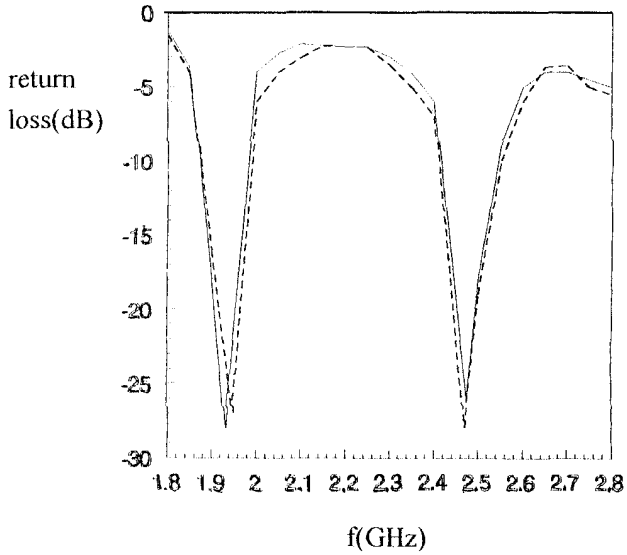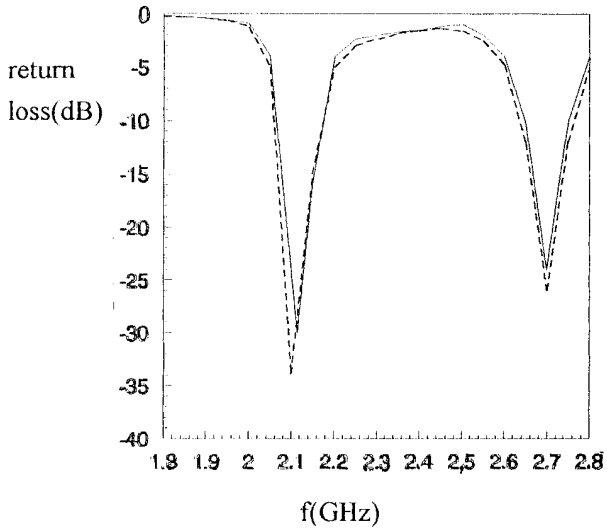
(a)

(b)

Figure 3. Comparisons with experimental results in [29]. $a = 6.9\,\text{cm}$, $h = 5.5\,\text{cm}$, $l = 1.8\,\text{cm}$, $W = 2.6\,\text{cm}$, $h = 0.159\,\text{cm}$, $\varepsilon_r = 2.5$ Measured: ————; Theory: - - - - - -.

(a)

(b)

Figure 4. Comparisons with experimental results in [15].
(a) $a = 2.55\,\text{cm},\ h = 3.32\,\text{cm}, l = w = 0.9\,\text{cm},\ h = 0.16\,\text{cm},\ \varepsilon_r = 4.4$
(b) $a = 2.55\,\text{cm},\ h = 3.32\,\text{cm}, l = w = 0.0\,\text{cm},\ h = 0.16\,\text{cm},\ \varepsilon_r = 4.4$
Measured: ———; Theory: - - - - - -.
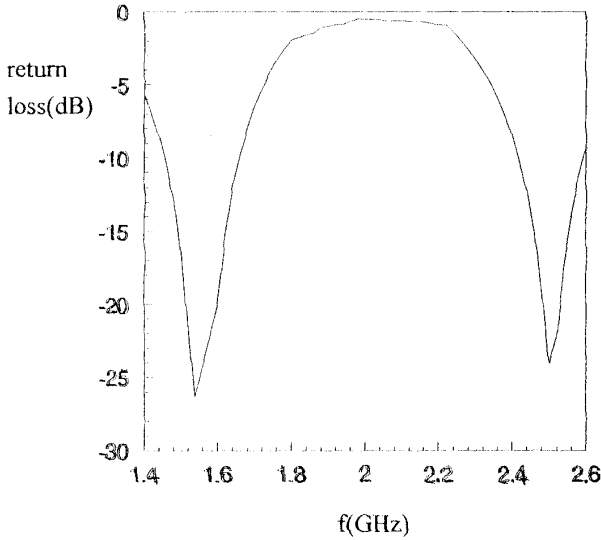
Figure 5. Return loss against frequency for the rectangular slot loaded patch. $a = 2.55\,\text{cm}$, $b = 3.32\,\text{cm}$, $l = 1.875\,\text{cm}$, $w = 0.9\,\text{cm}$, $h = 0.16\,\text{cm}$, $\varepsilon_r = 4.4$.

loaded antenna in [15] achieves a size reduction of $\sim 17\%$ and further reductions are impossible due to poor impedance matching characteristics at both bands, as stated in [15]. To realize greater antenna-size reduction, a $45°$-rotated square slot is also proposed in [15]. However, no significant improvement is observed. In present case, good impedance matching characteristics are achieved at both bands and a much larger antenna-size reduction is achieved. This shows the advantages of present antenna. It is due to more freedoms of tuning when a rectangular slot is used instead of a square slot. In fact, through loading of a rectangular slot in the center and proper location of the feed point, antenna-size reduction larger than $\sim 33\%$ with good impedance characteristics at both bands are also possible by further tuning the length and width of the slot and patch suitably.

From the FDTD simulation, it is found that the resonant frequency for TM_{10}, mode decreases with increasing slot length. The change of slot width affects the resonant frequency for TM_{10}, mode very little, but the input impedance changes with the slot width. Similarly, the resonant frequency for TM_{01} mode is decreased with the increase of slot width, but the change of slot length has few effects on it. To understand more about the characteristics of the slot-loaded antenna, it would be very helpful if the electric current distributions on the microstrip patch could be given. For comparisons, both the slot-loaded patch and the simple patch without slot are studied. Figure 6 shows the electric current distributions on the simple patch without slot at 2.115 GHz. Both the J_x and J_y are shown. Figure 7 shows the electric current distributions on the simple patch without slot at 2.698 GHz. For clear illustration, the maximum amplitude of the dominant current is normalized to 1. These current distributions clearly show the resonant conditions at TM_{10} and TM_{01} modes respectively.

Figure 8 shows the electric current distributions on the slot-loaded patch at 1.54 GHz. Compared with Figure 6, it is seen that the electric distributions J_x and J_y are strongly modified by the slot loading. This modified electric current distributions lead to the decrease of the resonant frequency. Figure 9 shows the electric current distributions on the slot-loaded patch at 2.50 GHz. It is also seen that the electric distributions are quite different from the distributions shown in Figure 7.

Because of the different electric current distributions on the slot-loaded patch and the simple patch without slot, their radiation patterns are expected to be different. These are shown in Figure 10. Figure 10(a) shows the E-plane radiation patterns for the slot-loaded antenna at 1.54 GHz and the simple patch at 2.115 GHz. Figure 10(b) shows the H-plane radiation patterns for the slot-loaded antenna at 1.54 GHz and the simple patch at 2.115 GHz respectively. It is seen that with slot loading, the radiation patterns are broadened at both planes. The extent of broadening is larger in the E plane than that in the H plane. Similar conclusions are drawn from the comparisons between the slot-loaded antenna at 2.50 GHz and the simple antenna at 2.698 GHz. Their patterns are omitted for brevity.
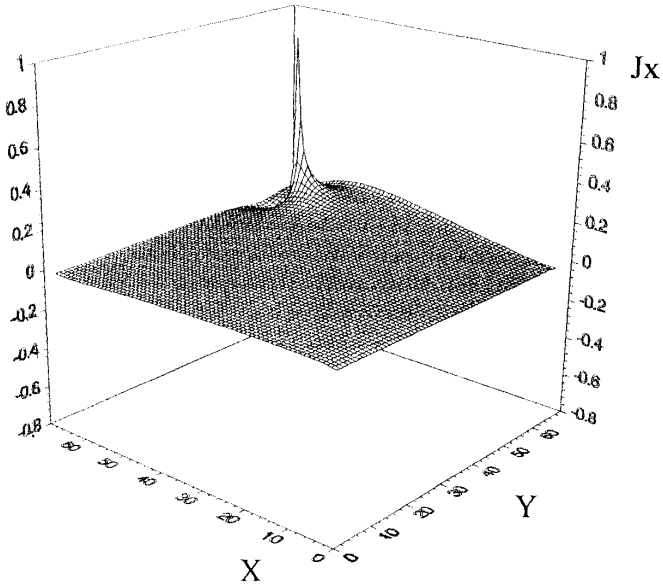
(a)
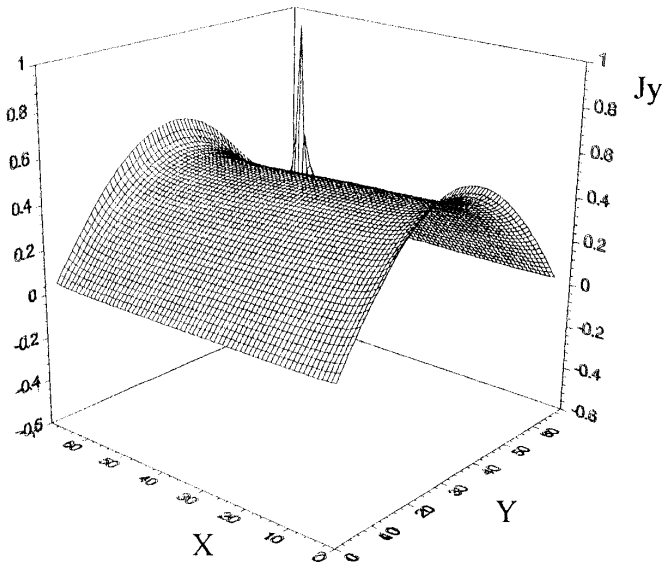
(b)

Figure 6. Electric current distributions for simple patch. Parameters same as that in Figure 4(b), $f = 2.115\,\text{GHz}$. (a) J_x; (b) J_y.
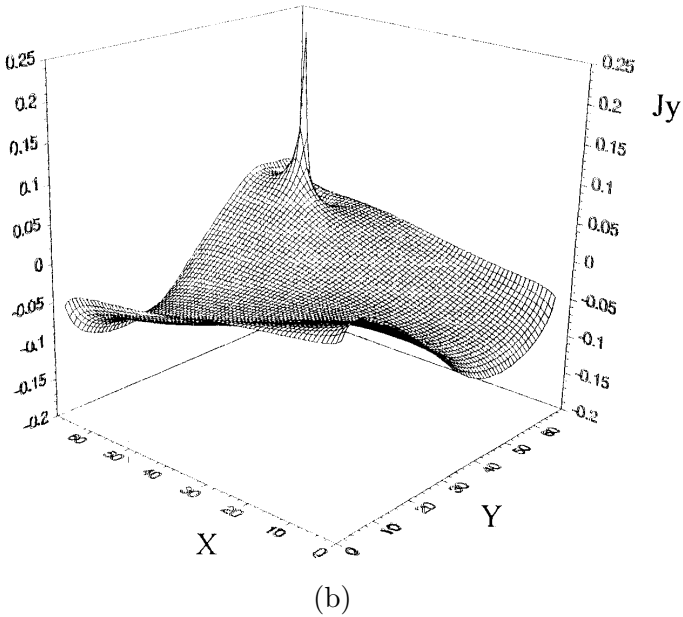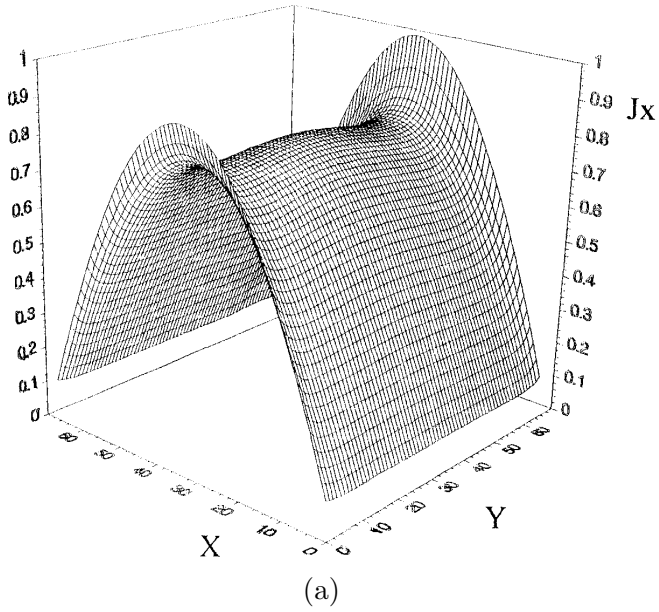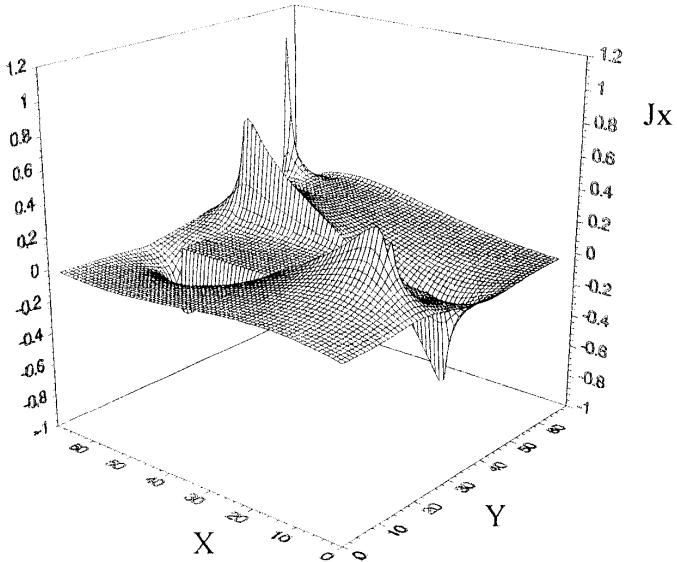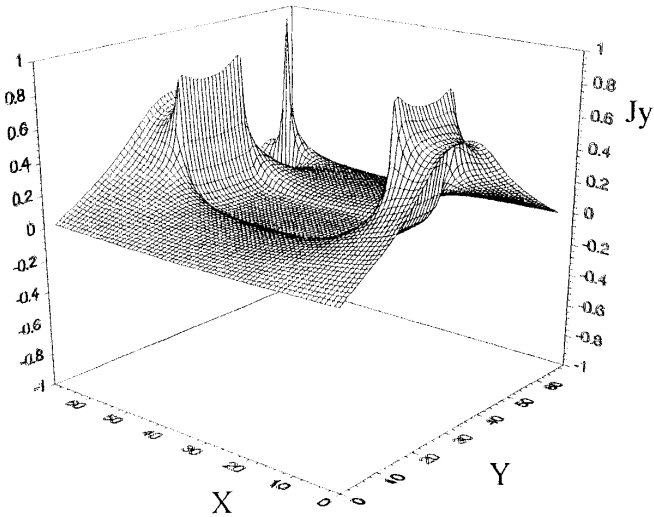
(a)

(b)

Figure 7. Electric current distribution for simple patch. Parameters same as that in Figure 4(b), $f = 2.698\,\mathrm{GHz}$. (a) J_x; (b) J_y.
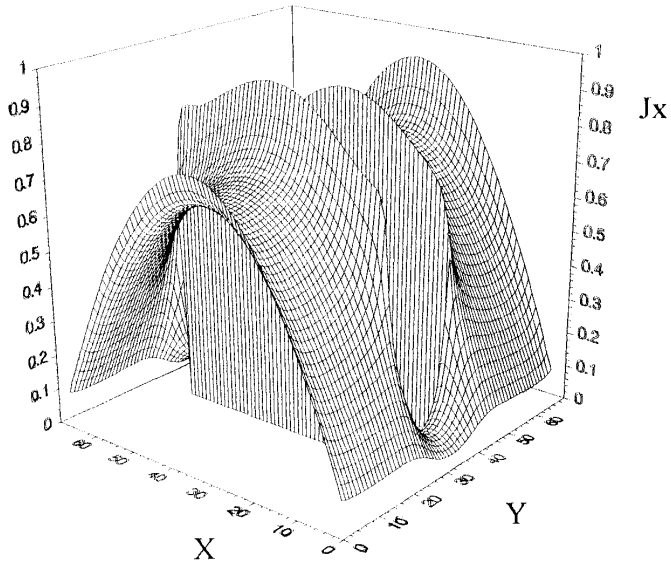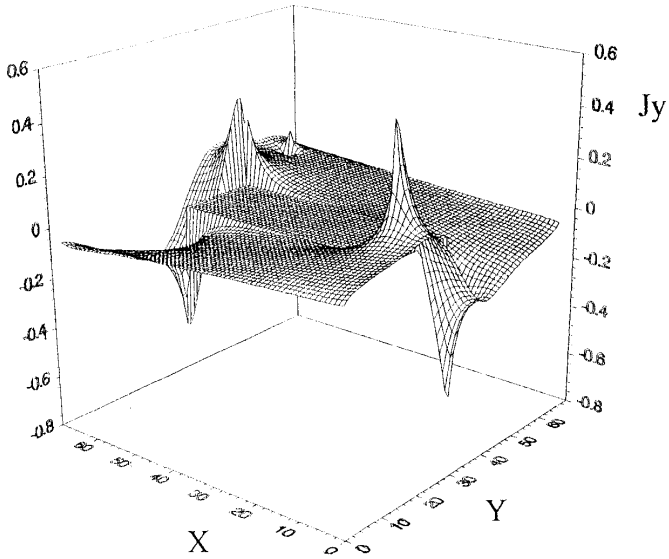
(a)

(b)

Figure 8. Electric current distribution for the rectangular slot loaded patch. Parameters same as that in Figure 5, $f = 1.54\,\text{GHz}$. (a) J_x; (b) J_y.
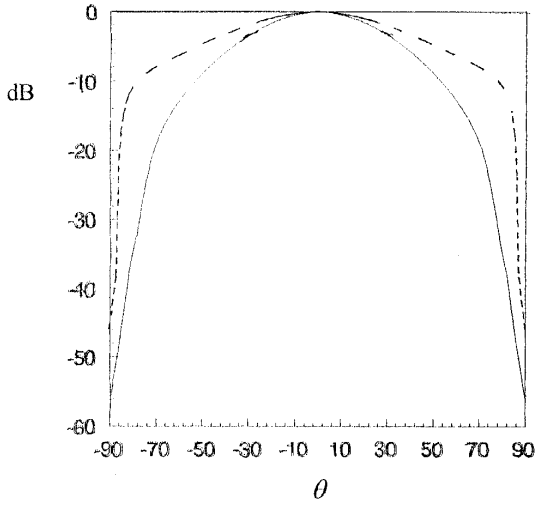
(a)

(b)

Figure 9. Electric current distribution for the rectangular-slot loaded patch. Parameters same as that in Figure 5, $f = 2.50\,\mathrm{GHz}$. (a) J_x; (b) J_y.

(a)
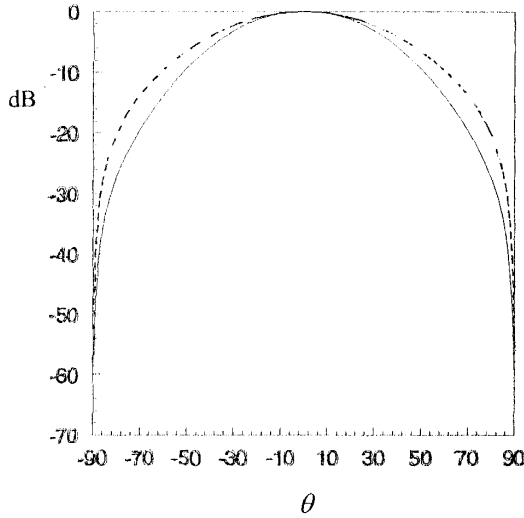
(b)

Figure 10. Comparisons between the radiation patterns.
(a) E-plane patterns for the rectangular-slot loaded antenna at
1.54 GHz and the simple patch at 2.115 GHz.
(b) H-plane patterns for the rectangular-slot loaded antenna at
1.54 GHz and the simple patch at 2.115 GHz.
Slot loaded patch (parameters as that in Figure 5: - - - - - -
Simple patch (parameters as that in Figure 4(b): ————

4. CONCLUSIONS

In this paper, a new size-reduced, dual-frequency antenna is studied, which is single probe-fed, rectangular microstrip patch with a rectangular slot cut in the center. The FDTD method is developed for the full-wave analysis of the antenna. A simple and accurate feed model is proposed, together with a simple method of calculating the radiation patterns. It is shown that through loading of the rectangular slot and proper location of the feed point, dual-frequency operations can be realized with an antenna- size reduction of $\sim 33\%$. Good impedance matching characteristics at both bands are also shown to be achieved. Further antenna-size reductions are possible by tuning the length and width of the slot and the patch. Electric current distributions on the rectangular patch for both the slot-loaded case and the case without slot are given, together with their radiation patterns. It is seen that the electric current distributions are strongly modified by the slot. The radiation patterns are broadened with slot loading. Theoretical analysis is verified by experimental results.

REFERENCES

1. Dahele,J. S., K. F. Lee, and D. P. Wong, "Dual-frequency stacked annular-ring microstrip antenna," *IEEE Trans. Ant. Propagat.*, Vol. AP-35, No. 11,1281–1285, Nov. 1987.
2. Wang, J., R. Fralich, C. Wu, and J. Litva, "Multifunctional aperture coupled stacked antenna," *Electron. Lett.*, Vol. 26, No. 25, 2067–2068, 1990.
3. Mirshekar-Syankal, D., and H. R. Hassani, "Characteristics of stacked rectangular and triangular patch antennas for dual band applications," *IEE 8th ICAP*, Edinburgh, March 1993.
4. Croq, F., and D. M. Pozar, "Multifrequency operation of microstrip antennas using aperture coupled parallel resonators," *IEEE Trans. Ant. Propagat.*, Vol. AP-40, No. 11, 1367–1374, Nov. 1992.
5. Richards, W. F., S. E. Davidson, and S. A. Long, "Dual-band reactively loaded microstrip antenna," *IEEE Trans. Ant. Propagat.*, Vol. AP-33, No. 5, 556-560, May 1985.
6. Davidson, S. E., S. A. Long, and W. F. Richards, "Dual-band microstrip antenna with monolithic reactive loading," *Electron. Lett.*, Vol. 21, No. 21, 936–937, 1985.

7. Waterhouse, R. B., and N. V. Shuley, "Dual frequency microstrip rectangular patches," *Electron. Lett.*, Vol. 28, No. 7, 606–607, 1992.

8. Zhong, S. S., and Y. T. Lo, "Single element rectangular microstrip antenna for dual frequency operation," *Electron. Lett.*, Vol. 19, No. 8, 298–300, 1983.

9. Schaubert, D. H., F. G. Ferrar, A. Sindoris, and S. T. Hayes, "Microstrip antennas with frequency agility and polarization diversity," *IEEE Trans. Ant. Propagat.*, Vol. AP-29, No. 1, 118–123, Jan. 1981.

10. Maci, S., G. Biffi Gentili, P. Piazzesi, and C. Salvador, "Dual-band slot-loaded patch antenna," *IEE Proc. Microw. Antennas Propag.*, Vol. 142, No. 3, 225–232, June 1995.

11. Piazzesi, P., S. Maci, and G. Biffi Gentili, "Dual-band, dual-polarized patch antennas," *Int. J. MlMCAE*, Vol. 5, No. 6, 375–384, 1995.

12. Wang, B. F., and Y. T. Lo, "Microstrip antenna for dual-frequency operation," *IEEE Trans. Ant. Propagat.*, Vol. AP-32, No. 9, 938–943, Sept. 1984.

13. Chen, J. S., and K. L. Wong, "A single-layer dual-frequency rectangular microstrip patch antenna using a single probe feed," *Microw. Opt. Technol. Lett.*, Vol. 11, 83–84, 1996.

14. Antar, Y. M. M., A. Ittipiboon, and A. K. Bhattacharyya, "A dual-frequency antenna using a single patch and an inclined slot." *Microw. Opt. Technol. Lett.*, Vol. 8, 309–311, 1995.

15. Chen, W. S., "Single-feed dual-frequency rectangular microstrip antenna with square slot," *Electron. Lett.*, Vol. 34, No. 3, 231–232, 1998.

16. Yee, K. S., "Numerical solution of initial boundary value problems involving Maxwell's equations in isotropic media," *IEEE Trans. Ant. Propagat.*, Vol. AP-14, No. 5, 302–307, May 1966.

17. Taflove, A., and M. E. Brodwin, "Numerical solution of steady state electromagnetic scattering problems using the time-dependent Maxwell's equations," *IEEE Trans. Microw. Theory Tech.*, Vol. MTT-23, No. 8, 623–630, Aug. 1975.

18. Reimeix, A., and B. Jecko, "Analysis of microstrip patch antennas using finite difference time domain method," *IEEE Trans. Ant. Propagat.*, Vol. AP-37, No. 11, 1361-1369, Nov. 1989.

19. Sheen, D. M., S. M. Ali, M. D. Abowzahra, and J. A. Kong, "Application of the three- dimensional finite-difference time-domain method to the analysis of planar microstrip circuit," *IEEE Trans. Microw. Theory Tech.*, Vol. MTT-38, No. 7, 849–857, July 1990.

20. Zhang, X., and K. K. Mei, "Time-domain finite difference approach to the calculation of the frequency-dependent characteristics of microstrip discontinuities," *IEEE Trans. Microw. Theory Tech.*, Vol. MTT-36, No. 12, 1775–1787, Dec. 1988.

21. Liao, Z. P., H. L. Wong, G. P. Yang, and Y. F. Yuan, "A transmitting boundary for transient wave analysis," *Scientia Sinica*, Vol. 28, No. 10, 1063–1076, Oct. 1984.

22. Mei, K. K., and J. Fang, "Superabsorption–A method to improve absorbing boundary conditions," *IEEE Trans. Ant. Propagat.* Vol. AP-40, No. 9, 1001–1010, Sept. 1992

23. Luebbers, R., L. Chen, T. Uno, and S. Adachi, "FDTD calculation of radiation patterns,impedance,and gain for a monopole antenna on a conducting box," *IEEE Trans. Ant. Propagat.*, Vol. AP-40, No. 12, 1577–1583, Dec. 1992.

24. Jensen, M., and Y. Rahmat-Samii, "Performance analysis of antennas for hand- held transceivers using FDTD," *IEEE Trans. Ant. Propagat.*, Vol. AP-42, No. 8, 1106–1113, Aug. 1994.

25. Wu, C., K. Wu, Z. Bi, and J. Litva, "Accurate characteristics of planar printed antenna using finite-difference time domain method," *IEEE Trans. Ant. Propagat.*, Vol. AP-40, No. 5, 526–533, May 1992.

26. Tirkas, P. A., and C. A. Balanis, "Finite difference time domain method for antenna radiation," *IEEE Trans. Ant. Propagat.*, Vol. AP-40, No. 3, 334–340, Mar. 1992.

27. Balanis, C. A., *Antenna Theory: Analysis and Design*, New York: Wiley, 1982.

28. James, J. R., and P. S. Hall ed., *Handbook of Microstrip Antennas*, Peter Peregrinus, 1989.

29. Palanisamy, V., and R. Garg, "Analysis of arbitrarily shaped microstrip patch antennas using segmentation technique and cavity model," *IEEE Trans. Ant. Propagat.*, Vol. AP-34, 1208–1213, 1986.

30. Luebbers, R.J., and H. S. Langdon, "A simple feed model that reduces time steps needed for FDTD antenna and microstrip calculations," *IEEE Trans. Ant. Propagat.,* Vol. AP-44, 1000–1005, 1996.